Electronic Supplementary Material (ESI) for Lab on a Chip.

SUPPLEMENTARY TABLES

Table S1: Oxygen diffusivity of common plastics (inspired from Rivera [1], Sheidaei [2])

Materials	Oxygen diffusion coefficient (cm^2/s)
PDMS	$3,4 \times 10^{-5}$
PEEK	$1,4 \times 10^{-6}$
PTFE	$2,8 \times 10^{-7}$
PMMA	$2,7 \pm 0,2 \times 10^{-8}$
COC	$4,6 \times 10^{-8}$

SUPPLEMENTARY FIGURES

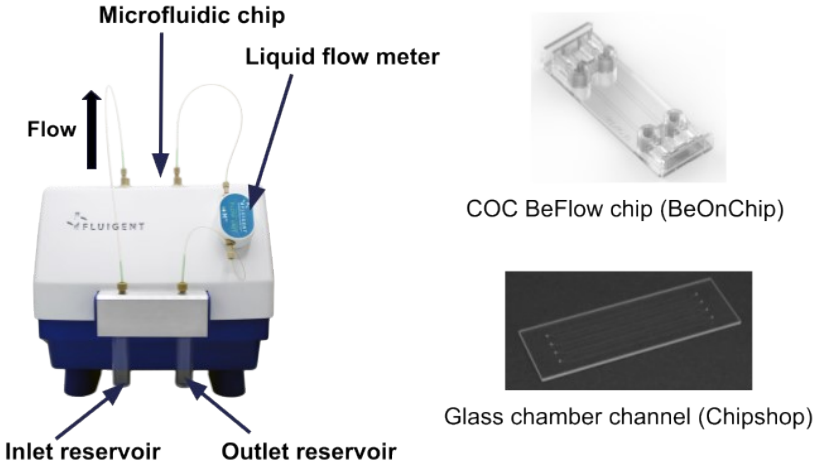

Figure S1: Photograph of Oxalis and of the commercial chips used: BeFlow (BeOnChip) and Chamber Channel (Chipshop).

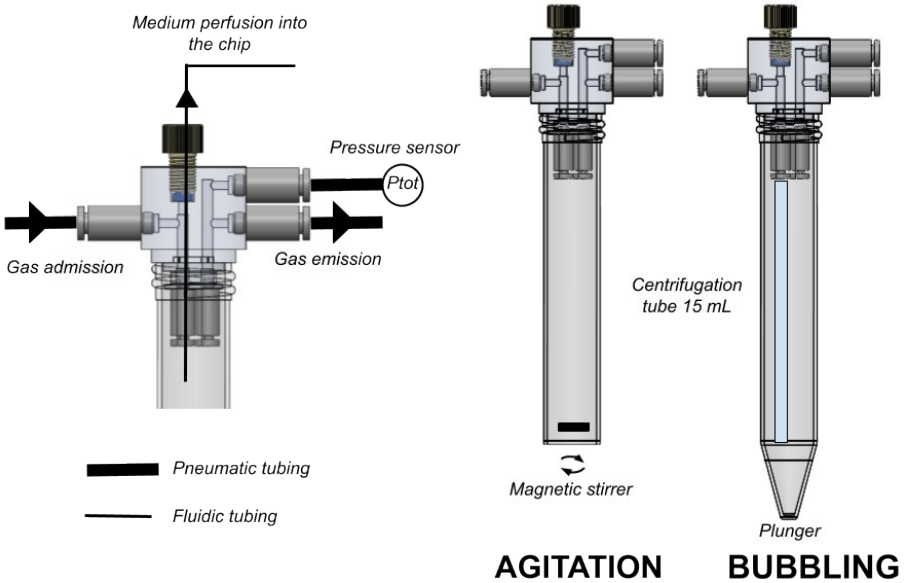

Figure S2: Custom Lid with three pneumatic inlets for pressure sensor, gas admission, gas emission, and one fluidic outlet to connect to the microfluidic chip. Two methods can be used to equilibrate the liquid cell culture medium: either agitating with a magnetic stirrer or bubbling with a plunger.

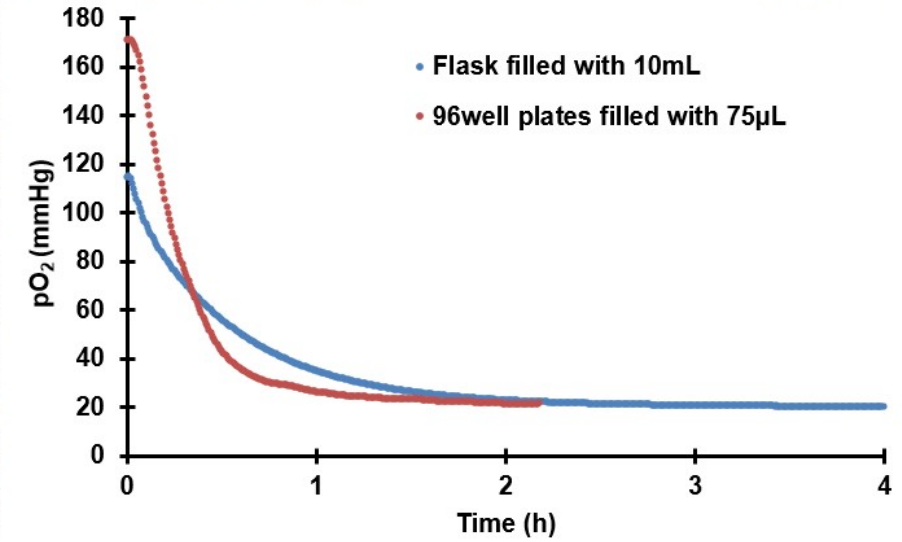

Figure S3: Oxygen equilibration of cell culture medium in an hypoxic incubator. Two conditions were compared: a T75 flask filled with 10mL of complete DMEM and a well of a 96well plates filled with 75µL of complete DMEM.

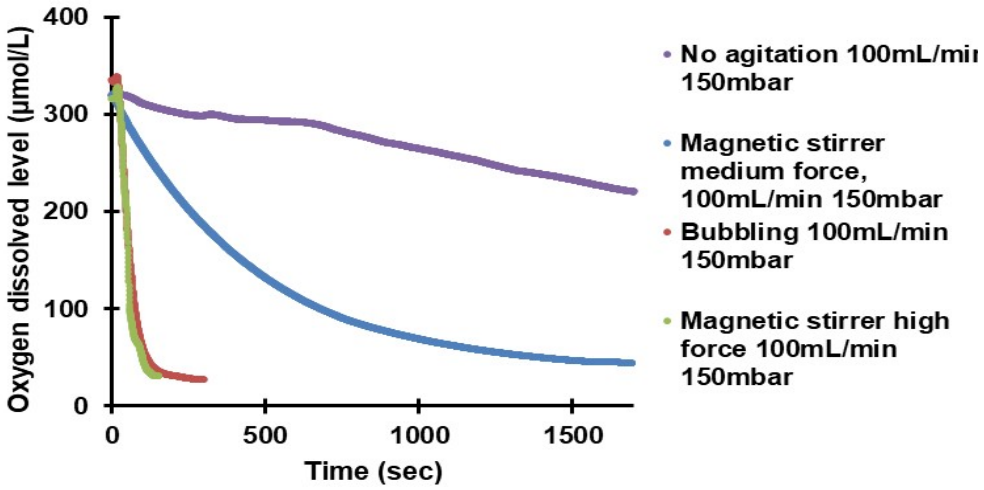

Figure S4: Desoxygenation of cell culture medium (DMEM without FBS, without PS) for a target of 20µmol/L (15mmHg). We compared two methods: using either bubbling, either a magnetic stirrer (reference : FisherBrand 10517) with different stirring forces (1 to 8, 8 corresponding to high force). Gas mix contains 1.9% oxygen and 5% CO_2.

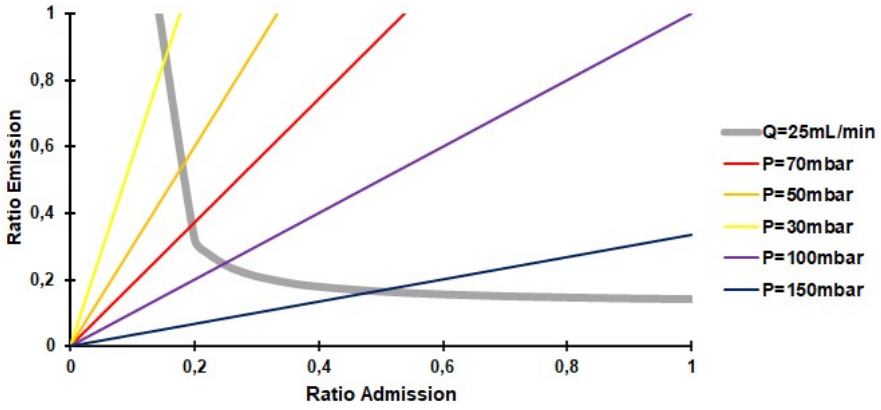

Figure S5: Intersection of iso-pressure and iso-flowrate curves. To be able to scan various pressures (P_{in}) we chose a Q_{gas} of 25mL/min.

Changing the opening ratio of the two valves will allow to scan different flow rates. The theoretical relationship between admission ratio (K_a), emission ratio (K_e) and flow rate (Qtot), in steady state conditions is described by the equation (1i) (plotted Fig. 2B) :

$$K_e = \frac{\frac{Pmax - Patm}{Qmax}}{\frac{Pmax - Patm}{Qtot} - \frac{Pmax - Patm}{K_a * Qmax}} \quad (1i)$$

With Pmax being the input gas pressure [bar] (set by the bottle manual pressure regulator), Patm being the outlet pressure of the emission valve, Qmax being the maximal flow rate achievable with this pressure [mL/min] for a complete opening of the valve, and Qtot being the flow rate accessible with different couple of (K_e, K_a).

These iso flow-rate curves were confirmed experimentally by scanning different opening couples of (emission valve, admission valve), as shown Fig. 2B. Similarly, changing the opening ratio of the two valves will allow to scan different flow rates according to the theoretical equation below (plotted Fig. 2C):

$$K_e = K_a * \left(\frac{Pmax - Pout_{gas}}{Ptot - Pout_{gas}} - 1 \right) \quad (1ii)$$

With Pin being the pressure accessible with different couple of (K_e,K_a). These iso pressure curves were confirmed experimentally, as shown Fig. 2C.

Finally, one can notice that below Pmax/2, Qtot is poorly affected by a change in Ke while it strongly depends on Ka.This is graphically visible at the upper left section of the graph (below Pmax/2), where the iso-flow rate curves are almost vertical. As a consequence, if the target pressure is lower than Pmax/2, fixing an opening of the admission valve (admission aperture) will mainly determine the flow rate, while pressure can be changed by modulating the opening of the emission valve (emission aperture).

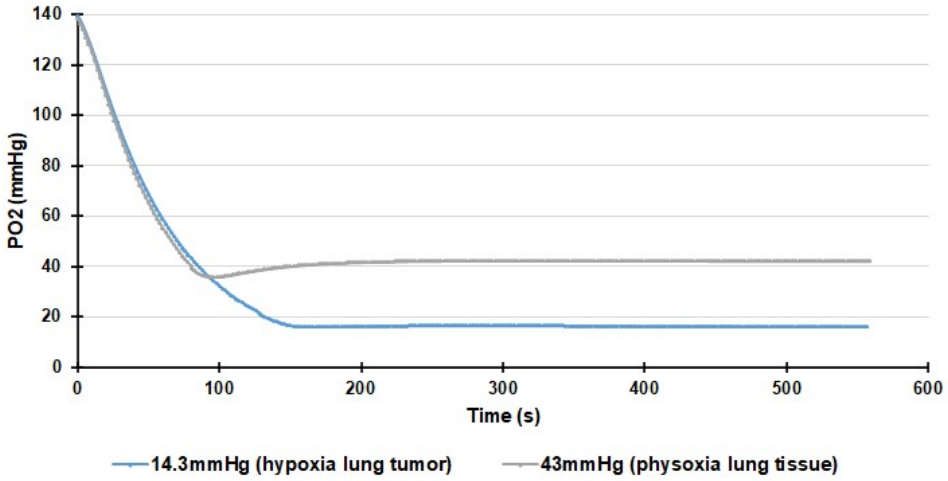

Figure S6: Oxalis allowed to reach at 37°C in 3mL DMEM a PO_2 target in less than 200sec with a precision of 2mmHg (N=3).

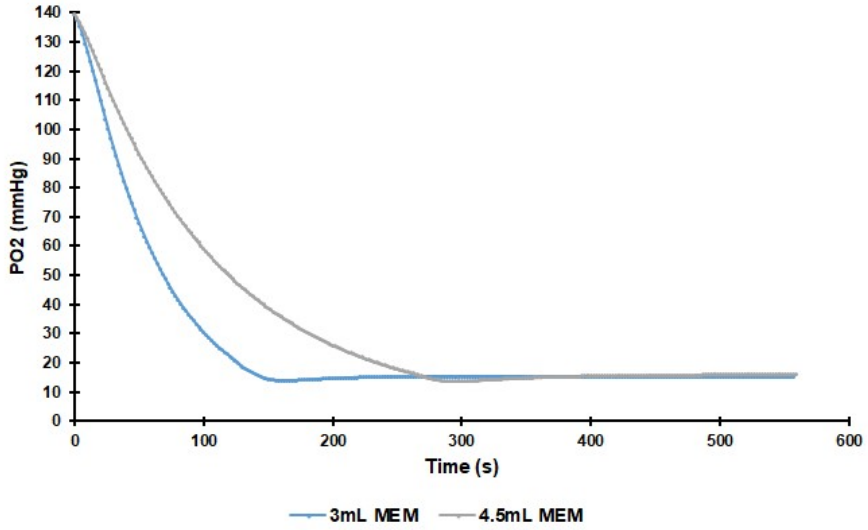

Figure S7: Increasing the volume in the reservoir increased slightly the equilibration time, for MEM at 37°C.

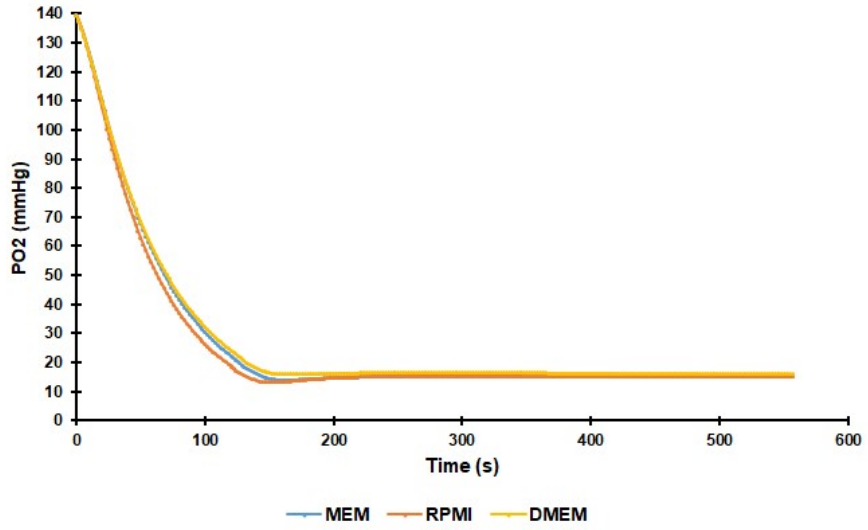

Figure S8: No significant differences in term of final values and dynamic were observed for 3mL of different cell culture medium (N=6): DMEM, MEM, RPMI.

The water vapor pressure influences the oxygen partial pressure of air-saturated water and water vapor-saturated air. Moreover, temperature variations strongly affect water vapor pressure, and thus influence the oxygen partial pressure. For example, the water vapor pressure is 47 mmHg if we culture the cells at 37°C in a conventional humid incubator [12]. To prevent from any variations of water vapor pressure, we keep the system at constant temperature (37°C) without humidity. Humidity is indeed not needed as we are continuously perfusing the microfluidic chip and working with low permeability materials preventing from evaporation.

Increasing the salt concentration leads to a decrease in oxygen solubility[13], which is known as the "salting-out effect". To quantify the salt concentration, the term salinity is often used and is expressed by: S = 1.805[Cl-] + 0.03 where S is the salinity in [%] [14]. As shown Fig. S5, we tested various common cell culture medium (DMEM, MEM, RPMI) with different salinity (respectively: [NaCl]=6400mg/L thus S=11.5, [NaCl]=6800mg/L thus S=12.3 and [NaCl]=6000mg/L thus S=10.9).

SUPPLEMENTARY EQUATIONS: PH CONTROL

$$NaHCO_3 \Leftrightarrow Na^+ + HCO_3^-$$
$$CO_2(s) + H_2O \Leftrightarrow H_2CO_3 \Leftrightarrow H^+ + HCO_3^-$$

According to Henderson-Hasselbach:

$$pK_A = -\log_{10}([HCO_3^-] * \frac{[H^+]}{[H_2CO_3^-]}) = pH - \log_{10}(\frac{[HCO_3^-]}{[H_2CO_3^-]})$$

At 37°C, the pK_A of H_2CO_3 is 6.1. According to Henry's law: $[CO_2(aq)] = pCO_2 \times k$, with k the Henry's constant, and $[H_2CO_3] = [CO_2(aq)]$. Although it is quite difficult to find precise sources about Henry's constant in cell culture medium, we consider Blombach et al.[11] study which defines k as $H_{CO2}(T = 20°C) = 40$ mmol/barL and $H_{CO2}(T = 37°C) = 25$ mmol/bar.L.

The only value that we know is $[NaHOC_3]$ (= $[HCO_3^-]$) in cell culture medium, as the informations can be find in any formulation description. To conclude, for an initial amount of $[HCO_3^-]_I$:

$$pH = 6.1 + \log_{10}(\frac{NaHCO_3}{84.007 * 0.00024 * \%CO_2} - 1)$$

Or we can express it as a function of pCO_2 and P_{in}:

$$pH = 6.1 + \log_{10}(\frac{Pin * 51.98 * NaHCO_3}{100 * pCO_2} - 1)$$

1 S. F. Lam, V. S. Shirure, Y. E. Chu, A. G. Soetikno and S. C. George, *PLoS One*, 2018, **13**, 1–16.

2 K. R. Rivera, V. A. Pozdin, A. T. Young, P. D. Erb, N. A. Wisniewski, S. T. Magness

and M. Daniele, *Biosens. Bioelectron.*, 2019, **123**, 131–140.
3 S. Martewicz, G. Gabrel, M. Campesan, M. Canton, F. Di Lisa and N. Elvassore, *Anal. Chem.*, 2018, **90**, 5687–5695.
4 Y. Gao, G. Stybayeva and A. Revzin, *Lab Chip*, 2019, **19**, 306–315.
5 F. Tonon, G. G. Giobbe, A. Zambon, C. Luni, O. Gagliano, A. Floreani, G. Grassi and N. Elvassore, *Sci. Rep.*, 2019, **9**, 1–10.
6 R. Koens, Y. Tabata, J. C. Serrano, S. Aratake, D. Yoshino, R. D. Kamm and K. Funamoto, *APL Bioeng.*, 2020, **4**, 016106.
7 V. S. Shirure, S. F. Lam, B. Shergill, Y. E. Chu, N. R. Ng and S. C. George, *Lab Chip*, 2020, **20**, 3036–3050.
8 S. Barmaki, D. Obermaier, E. Kankuri, J. Vuola, S. Franssila and V. Jokinen, *Micromachines*, , DOI:10.3390/mi11110979.
9 V. Palacio-Castañeda, L. Kooijman, B. Venzac, W. P. R. Verdurmen and S. Le Gac, *Micromachines*, 2020, **11**, 382.
10 I. Berger Fridman, G. S. Ugolini, V. Vandelinder, S. Cohen and T. Konry, *Biofabrication*, , DOI:10.1088/1758-5090/abdb88.
11 B. Blombach and R. Takors, *Front. Bioeng. Biotechnol.*, 2015, **3**, 1–11.
12 R. Wenger, V. Kurtcuoglu, C. Scholz, H. Marti and D. Hoogewijs, *Hypoxia*, 2015, 35.
13 W. Xing, M. Yin, Q. Lv, Y. Hu, C. Liu and J. Zhang, *Oxygen Solubility, Diffusion Coefficient, and Solution Viscosity*, Elsevier B.V., 2014.
14 M. Fernandez, *Salinity characteristics and distribution and effects of alternative plans for freshwater withdrawal*, 1985.